ACS Catalysis

Letter

Cite This: ACS Catal. 2018, 8, 2735−2740

pubs.acs.org/acscatalysis

Highly Selective Nonoxidative Coupling of Methane over Pt-Bi Bimetallic Catalysts

Yang Xiao and Arvind Varma*

Davidson School of Chemical Engineering, Purdue University, West Lafayette, Indiana 47907-2100, United States

Supporting Information

ABSTRACT: There is widespread interest in converting methane, primary component of natural gas and shale gas, into valuable chemicals. As an important direct methane transformation technique, despite extensive research conducted for decades, oxidative coupling of methane (OCM) remains industrially uneconomical owing to low selectivity toward valuable target products (C_2 species, ethane/ethylene). In the present work, we describe that ZSM-5 zeolite supported bimetallic Pt-Bi catalysts stably and selectively convert methane to C_2 species with high carbon selectivity (>90%) at relatively moderate temperatures (600−700 °C). On the basis of experimental observations, it is proposed that the surface Pt in the catalysts functions as the active site for methane activation, while Bi addition as promoter plays an important role in C_2 species formation and catalyst stability.

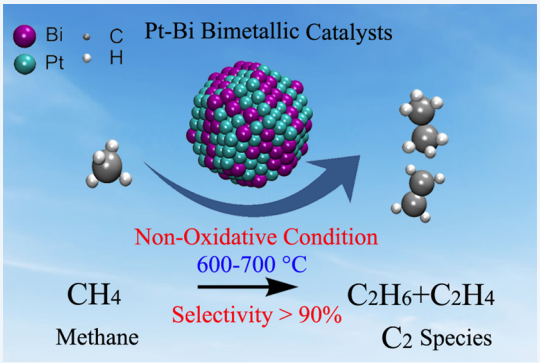

KEYWORDS: *shale and natural gas utilization, nonoxidative coupling of methane (NOCM), Pt-Bi bimetallic catalysts, high selectivity toward C_2 species, Bi promoter effect on C_2 species formation*

The abundance of methane, the main component of natural gas (~95%) and shale gas (typically >70%), on Earth makes it an attractive source for energy and chemicals for at least the next century. Catalytic transformation of methane to value-added chemicals plays an important role in methane utilization.[1,2] Various routes have been considered, including indirect transformation, which converts methane to syngas as an intermediate followed by its further conversion to other compounds, and direct transformation, which converts methane to higher hydrocarbons (e.g., ethylene, benzene) or oxygenates (e.g., methanol, formaldehyde) without any intermediate products.[3] Direct transformation is more attractive because it saves both operating costs and capital investment. Among direct transformation technologies, oxidative coupling of methane (OCM) is promising because the primary products (C_2 species, ethane/ethylene) are precursors for a variety of more valuable products: e.g., plastics and resins. Tuning the selectivity toward C_2 species in OCM, however, has been a longstanding challenge since the 1980s, owing to the unavoidable presence of overoxidized species (CO/CO_2) under oxidative conditions. Hundreds of catalyst candidates have been prepared and tested for OCM, while selectivity toward CO/CO_2 is typically about 50%, indicating uneconomical conversion of carbon atoms.[4]

Nonoxidative conversion of methane to aromatics, first reported in 1993,[5] improves carbon atom economy. Using Mo supported on zeolites, existing nonoxidative technologies generate benzene as the main product, but unavoidable coke formation limits the catalyst lifetime and process commercialization.[6] Although the selectivity toward benzene is typically about 80−90%, other aromatic hydrocarbons (C_7−C_9) as well as C_2 species (both ethane and ethylene) have also been reported.[7−9] In a recent report, 2−3% methane conversion was reached over Bi/SiO_2 at 900 °C under nonoxidative conditions, while the selectivity toward C_2 products was about 40%.[10]

Nonoxidative coupling of methane (NOCM) to form C_2 hydrocarbons has been considered since the 1990s. Extensive investigations have been focused on the two-step process, involving first feeding methane for dissociative adsorption on catalyst surface, followed by feeding hydrogen to generate higher hydrocarbons.[11−16] By only feeding methane continuously, Belgued et al.[17] reported that C_2H_6 and H_2 were immediately produced over a commercial 6 wt % Pt/SiO_2 catalyst at low temperature (250 °C), while owing to catalyst deactivation, both products disappeared for a time on stream (TOS) of more than 8 min. This indicates that methane can be activated at temperatures lower than those typically used in OCM (>700 °C). Soulivong et al.[18] showed that ethane with >98% carbon selectivity was produced over silica-supported tantalum hydride catalyst at temperatures <500 °C, although methane conversion was less than 0.5%. Guo et al.[19] reported 48% conversion of methane under nonoxidative conditions over Fe/SiO_2 catalyst at 950 °C, producing ethylene, benzene, and naphthalene with carbon selectivities of 53%, 22%, and 25%, respectively. Gerceker et al.[20] also found similar products

Received: January 12, 2018
Revised: February 9, 2018
Published: February 21, 2018

DOI: 10.1021/acscatal.8b00156
ACS Catal. 2018, 8, 2735−2740

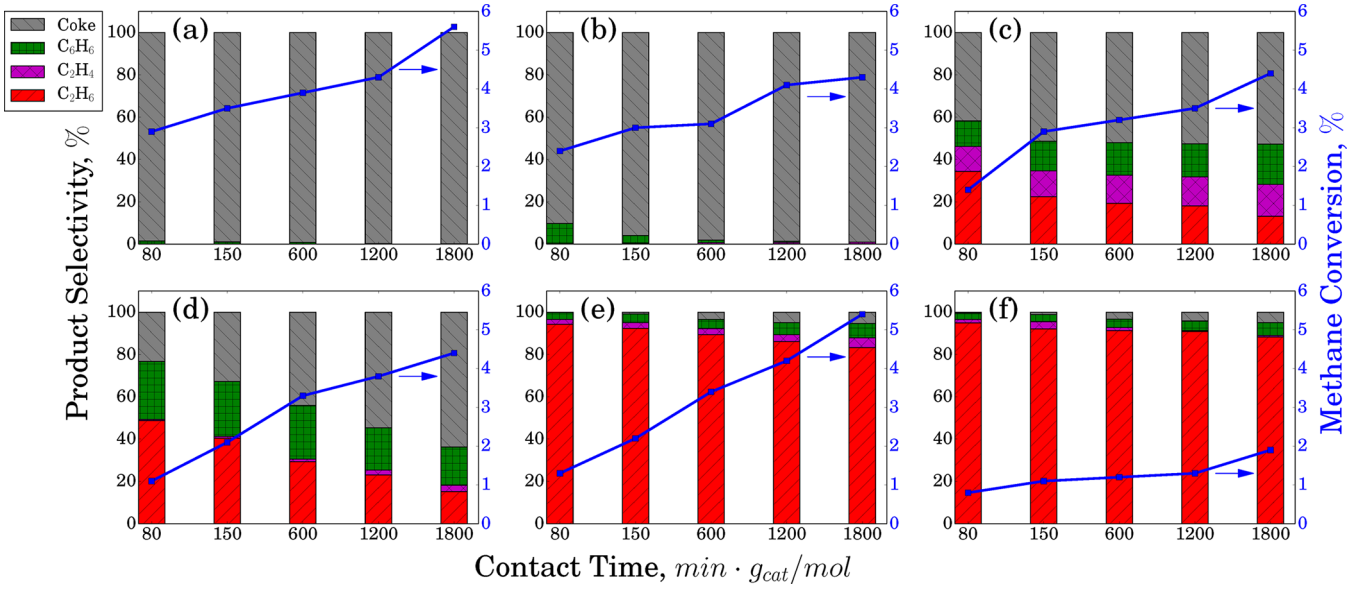

Figure 1. Product distribution at 650 °C and 0.1 atm methane partial pressure over (a) 1% Pt, (b) 1% Pt-0.1% Bi, (c) 1% Pt-0.2% Bi, (d) 1% Pt-0.5% Bi, (e) 1% Pt-0.8% Bi, and (f) 1% Pt-1% Bi catalysts.

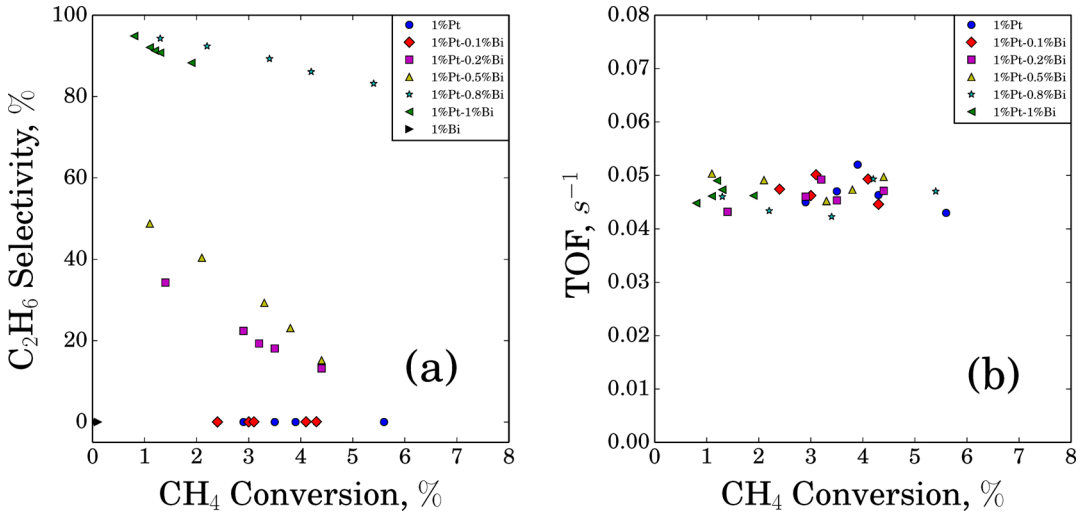

Figure 2. Performance of different Pt-Bi/ZSM-5 catalysts at various methane conversions for (a) ethane selectivity and (b) turnover frequency (TOF) at 650 °C and 0.1 atm methane partial pressure.

over PtSn catalyst supported on SiO_2 and ZSM-5 at 700 °C, however, the methane conversion was less than 0.3%.

In the present report, under nonoxidative conditions, we describe that Pt-Bi bimetallic catalysts supported on ZSM-5 zeolite selectively convert methane to ethane with high carbon selectivity (>90%) and typical methane conversion of ca. 2%, along with equivalent molar hydrogen generated as a byproduct. The catalyst exhibits little deactivation during an 8 h test, indicating good stability and prevention of coke formation. This is the first report of stable methane coupling in a continuous flow reactor, at relatively moderate temperatures (600−700 °C), with methane conversion ∼2% and carbon selectivity to C_2 hydrocarbon species >90%.

Various ZSM-5 zeolite supported Pt-Bi bimetallic catalysts were prepared, characterized, and tested in a fixed-bed reactor (see Materials and Methods in the Supporting Information). As noted in Materials and Methods, the Pt and Bi loadings were both by weight %, while H-ZSM-5 was the H-form ZSM-5 with an Si/Al ratio of 40. For brevity, in later sections the term weight % is not noted explicitly. These fresh catalysts exhibit similar BET surface areas (372−412 m^2/g), pore sizes (2.8−3.5 nm), pore volumes (0.33−0.41 cm^3/g) (Table S1), and Pt metal dispersions (22−29%) (Table S2). Tables S1 and S2 show that, for the used 1% Pt catalyst, all of these values dramatically decreased (BET surface area 234 m^2/g, pore size 1.3 nm, pore volume 0.14 cm^3/g, and metal dispersion 16%). For the used bimetallic 1% Pt-0.8% Bi catalyst, however, only a slight decrease was observed in these values (BET surface area 329 m^2/g, pore size 2.3 nm, pore volume 0.31 cm^3/g, and metal dispersion 20%). TEM scans (Figure S1) show that metals (dark dots) were successfully loaded on the ZSM-5 support and the metal dispersion (calculated by TEM-based particle size[21]) values were consistent with the H_2-O_2 titration[22] data in Table S2. The XRD patterns (Figure S2) for various Pt-Bi/ZSM-5 catalysts are compared to diffraction patterns for unsupported MFI (ZSM-5) reported in the International Zeolite Association

DOI: 10.1021/acscatal.8b00156
ACS Catal. 2018, 8, 2735−2740

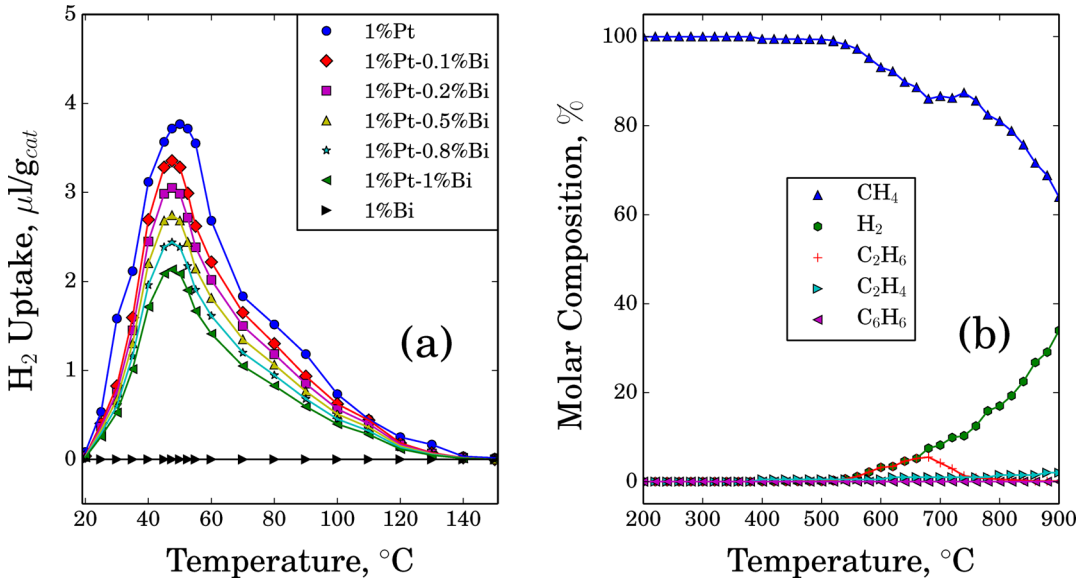

Figure 3. Temperature-programmed investigations: (a) H_2 desorption (H_2-TPD) from different Pt-Bi/ZSM-5 catalysts and (b) surface reaction (TPSR) profiles for 1% Pt-0.8% Bi/ZSM-5 catalyst at 0.1 atm methane partial pressure and 600 min g_{cat}/mol contact time.

(IZA) structure database.[23] Fresh supported (Figure S2a–g) and unsupported ZSM-5 (Figure S2h) exhibit similar patterns, likely due to low metal loading (1 wt % or less) and high Pt dispersion (20–30%).[24] The used 1% Pt catalyst (Figure S2i) exhibited fewer peaks in comparison to other materials, indicating that the crystallinity was changed slightly, likely owing to coke deposit. The used 1% Pt-0.8% Bi catalyst (Figure.S2j) showed the same MFI structure as well, implying less coke deposit and thus better stability in comparison to the pure Pt catalyst. Table S3 shows that the fresh and used catalysts contained essentially the same amounts of Pt and Bi as designed.

As shown in Figure 1, by varying the contact time of feed methane with packed catalysts, different methane conversions were obtained, as plotted by blue lines, while detailed product distributions are illustrated as bar charts. (Definitions for Methane Conversion, Product Selectivity and Yield in the Supporting Information). All methane conversions were less than 7%, limited by thermodynamic equilibrium under the operating conditions, corresponding to

$$CH_4 \rightarrow 0.5C_2H_6 + 0.5H_2 \quad (1)$$

$$CH_4 \rightarrow 0.5C_2H_4 + H_2 \quad (2)$$

For the 1% Pt catalyst, methane conversions were between 3% and 6%, while no hydrocarbon but only hydrogen was detected, owing to coke formation over the pure Pt surface.[25] For the 1% Pt-0.1% Bi catalyst, methane conversion was similar to results for the 1% Pt catalyst, with 0.5–8% benzene (C_6H_6) selectivity but no C_2 hydrocarbons generated. For four other bimetallic catalysts with 1% Pt and 0.1–1% Bi in Figure 1, ethane as the target product in the present work was produced with a variety of selectivity values ranging from 17% to 95%, while benzene and ethylene (C_2H_4) were formed as byproducts as well.

Figure 2a additionally shows that the selectivity toward ethane always decreased with an increase in methane conversion for these four catalysts. For the 1% Bi catalyst, on the other hand, no methane conversion (<0.1%) was found. In particular, for the 1% Pt-0.8% Bi catalyst, selectivity toward ethane was 85–95% when methane conversion was 1–5%. Note that equilibrium methane nonoxidative conversion to C_2 species is about 2–3% at 650 °C. (Thermodynamic Consideration and Figure S4 in the Supporting Information), while higher than equilibrium conversion was typically observed for methane nonoxidative conversion at short time on stream (TOS) in the literature.[7,8,26,27] For consistency, all data reported in our work for catalytic performance comparison were taken at 1 h TOS. As reported in the literature, Bi addition to Pt could tune catalytic activity, where Bi functions as site blocker,[28,29] while Bi alone shows poor catalytic activity. For increasing amounts of Bi addition to Pt, chemisorption of small molecules (e.g., H_2, CO,[30] and C_2H_4[31]) was found to be attenuated, indicating relatively lower activity for reaction and higher tolerance for poison species. Coverage values of chemisorbed species, influenced by both geometric and electronic effects,[32,33] also depend on molecular size, which indicates that, for a specific reaction, a particular Pt/Bi composition is favored. For example, Greeley et al.[34] reported that $Pt_{1.00}Bi_{0.95}$ exhibits excellent activity for hydrogen evolution, while our prior work described that 3% Pt-0.6% Bi provides the highest 1,3-dihydroxyacetone yield from glycerol selective oxidation.[35] In the present work, we observe that, for NOCM conversion, 1% Pt-0.8% Bi gives the best catalytic performance. Figure 2b shows that over various catalysts tested in Figures 1 and 2a, turnover frequencies (TOF) based on Pt surface dispersion (Table S2) and methane conversion were essentially constant (0.042–0.053 s^{-1}). This feature demonstrates that surface Pt is the active site for methane activation, as reported previously.[36]

H_2 temperature-programmed desorption (H_2-TPD) profiles in Figure 3a demonstrate that hydrogen uptake at room temperature was attenuated with increasing Bi addition to 1% Pt/ZSM-5. For 1% Bi catalyst, no hydrogen uptake was found, indicating an inactive nature for Bi as shown in Figure 2a. Temperature-programmed surface reaction (TPSR) profiles in Figure 3b describe that below 500 °C methane cannot be activated efficiently, owing to the chemical stability of the methane molecule. Between ca. 500 and 650 °C, methane was converted to equivalent molar amounts of ethane and

DOI: 10.1021/acscatal.8b00156
ACS Catal. 2018, 8, 2735–2740

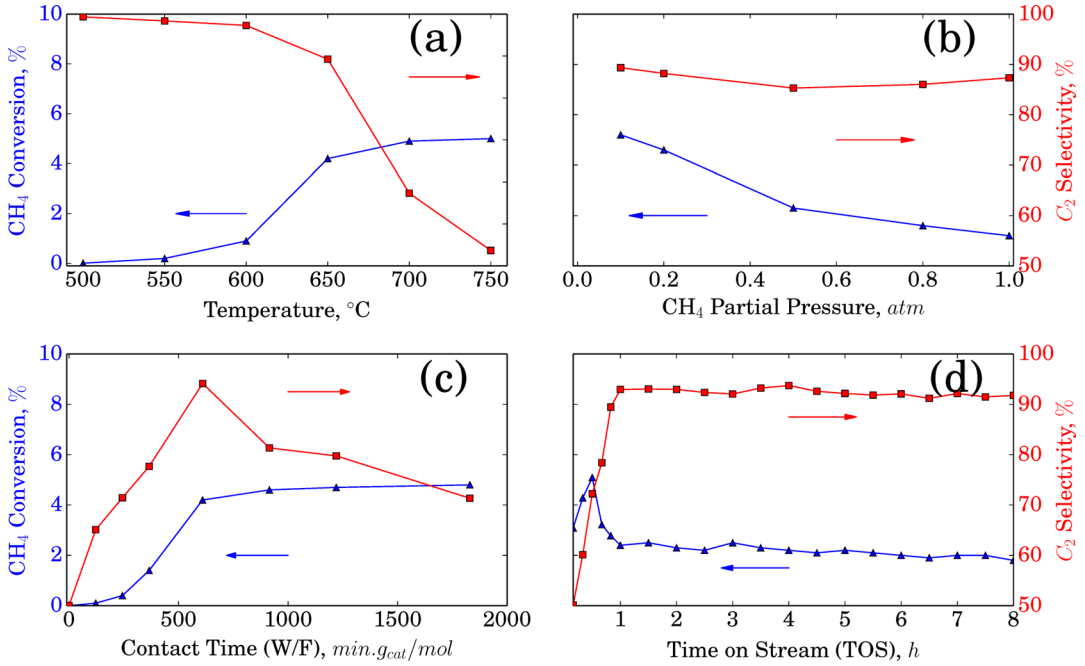

Figure 4. Effects of operating conditions and catalyst stability over 1% Pt-0.8% Bi: (a) temperature effect at 0.1 atm methane partial pressure and 600 min g_{cat}/mol contact time; (b) methane partial pressure effect at 650 °C and 600 min g_{cat}/mol contact time; (c) contact time effect at 0.1 atm methane partial pressure and 650 °C; (d) catalyst stability at 0.1 atm methane partial pressure, 650 °C, and 300 min g_{cat}/mol contact time.

hydrogen, as indicated by eq 1. From ca. 700 to 800 °C, methane conversion continued to increase, while ethane concentration decreased from ca. 2.5% to nearly 0. The hydrogen production rate from 700 to 900 °C, however, continued to increase, implying further dehydrogenation of methane and leading to coke formation. As reported in the literature,[25,36,37] not only initial activation of methane ($CH_4 \rightarrow CH_3 + H$) but also further dehydrogenation of methane (e.g., forming CH_2, CH, and C species) occurs over the Pt surface, owing to relatively low reaction barriers of C−H bond cleavage (<1 eV). Thus, in comparison to C−C coupling (reaction barrier typically >2 eV over a flat surface[38] and 1−2 eV over a step surface[39]), Pt catalysts preferably promote further dehydrogenation of methane rather than C−C coupling,[40] eventually forming coke, which is consistent with the 1% Pt curve in Figures 1 and 2a. In addition to the Pt surface, C−C coupling could also occur at acidic sites of ZSM-5, as reported previously.[41,42] Since the 1% Pt/ZSM-5 catalyst, as described in Figures 1 and 2, did not lead to any C_2 product, the acidic site in ZSM-5 appears to be inactive for C−C coupling in NOCM conversion in the present study. Ethane dehydrogenation to ethylene and/or acetylene could occur over pure Pt surfaces.[43,44] With the addition of a second metal to Pt, binding of molecules is typically weaker over bimetallic surfaces,[45,46] indicating relatively higher reaction barriers. As reported in the literature, a shorter contact time favors lower reactivity of ethane dehydrogenation.[47,48] These are likely reasons for the limited ethane dehydrogenation product in the present study.

Figure S3a,b shows temperature-programmed oxidation (TPO) profiles for used 1% Pt and used 1% Pt-0.8% Bi catalysts, respectively. Initial oxidation of used 1% Pt occurred at ca. 300 °C, followed by two clear peaks at 440 and 540 °C (see also Table S4). For used 1% Pt-0.8% Bi, however, only one distinguished peak was identified, although it was followed by slight dragging (indicating another small peak). As given in Table S4, by integrating curves in Figure S3, accumulated coke amounts were obtained. Table S5, demonstrating various coke amount calculation methods, indicates good mass balance. The used 1% Pt-0.8% Bi contained much less coke (27 mg/g_{cat}) than used 1% Pt (497 mg/g_{cat}). These observations suggest that by addition of Bi to Pt/ZSM-5 catalyst, methane was activated at relatively low temperature (600−700 °C), while further dehydrogenation of methane, leading to coke deposits, was suppressed owing to the less active Pt-Bi surface in comparison to the pure Pt surface.[49] In our prior works, Bi was used as a promoter for either tuning selectivity toward target products[35,50] or improving catalyst stability.[51] With the participation of guaiacol molecules over Pt-Bi catalysts, it was proposed that CH_4 decomposed on the Pt surface and methyls coupled to form ethane.[51] It appears that, in the present work, Bi addition to Pt combines these two functions: promoting NOCM selectivity to ethane and extending catalyst lifetime.

Figure 4a shows temperature effects on NOCM over the range 500−700 °C. Similar to the case for Figure 3b, methane conversion increased with temperature while ethane selectivity decreased, reaching a maximum ethane yield (selectivity × conversion) of 1.8% at 650 °C. For standard operating conditions (Materials and Methods), the methane partial pressure was 0.1 atm. Figure 4b shows that 0.1−1 atm of methane partial pressure gave essentially the same C_2 selectivity yet higher methane conversion at lower methane partial pressure. This feature occurs when thermodynamics dominates NOCM conversion (Thermodynamic Considerations and Figure S5 in the Supporting Information). Figure 4c illustrates the contact time effect on NOCM conversion. When a long contact time was used, the main byproduct was aromatic coke, although small amounts of ethylene and benzene were detected as well. It has been proposed that, in all nonoxidative conversions of methane, C_2 species were produced as intermediates for either higher hydrocarbon or coke formation.[7] Thus, methane conversion typically follows the reaction

DOI: 10.1021/acscatal.8b00156
ACS Catal. 2018, 8, 2735−2740

network series $CH_4 \rightarrow C_2H_6 \rightarrow C_xH_y$ ($x > 2$, $y \geq 0$). In the present work, since the intermediate C_2 species was the target product, as shown in Figure 4c, it exhibited a selectivity maximum at ca. 600 min g_{cat}/mol, as expected from kinetic analysis (Kinetic Considerations and Figure S6 in the Supporting Information). Figure 4d shows that, following an initial transient activation period, both methane conversion and selectivity toward ethane were stable over the entire 8 h test. Note that for longer TOS (24−48 h), methane conversion slowly dropped to ca. 1%, while ethane selectivity was still maintained at about >80%. In comparison to stable values at 1−8 h TOS, in the initial activation period it appears that methane conversion was higher (4−5%), while the ethane selectivity was lower (50−80%). This suggests that carbonaceous deposits occurred during the initial activation period. As reported in the literature, these deposits may contribute to nonoxidative dehydrogenation of light hydrocarbons.[52−55] This is the likely reason for irregular higher conversion than equilibrium values at short TOS, which was also observed in other methane nonoxidative conversion publications.[7,8,26,27] At long TOS, as shown in Figure 4d, the methane conversion decreased below equilibrium values.

In general, current technologies for direct transformation of methane are not followed industrially owing to inefficient carbon atom utilization. In the present report, we describe a heterogeneous catalytic process at relatively moderate temperatures (600−700 °C) for stable methane conversion into ethane with carbon selectivity >90% and methane conversion ∼2%. This is a promising start toward technologies suitable for exploitation on the industrial scale.

■ ASSOCIATED CONTENT

Supporting Information

The Supporting Information is available free of charge on the ACS Publications website at DOI: 10.1021/acscatal.8b00156.

Materials and methods, definitions for methane conversion, product selectivity, and yield, thermodynamic considerations, kinetic considerations, notation, and tables and figures as described in the text (PDF)

■ AUTHOR INFORMATION

Corresponding Author

*A.V.: e-mail, avarma@purdue.edu; tel, 765-494-8484; fax, 765-494-0805.

ORCID

Yang Xiao: 0000-0003-1705-2213

Arvind Varma: 0000-0002-3472-5929

Notes

The authors declare no competing financial interest.

■ ACKNOWLEDGMENTS

This work was supported by the Davidson School of Chemical Engineering, the R. Games Slayter and the William and Cynthia Smith gift funds. This paper is based upon work supported in part by the National Science Foundation under Cooperative Agreement No. EEC-1647722. Any opinions, findings and conclusions or recommendations expressed in this material are those of the authors and do not necessarily reflect the views of the National Science Foundation. We thank Ms Nuttanit Pramounmat for help with some catalyst characterization as well as Dr. Jeff T. Miller and Mr. Johnny Zhuchen for useful discussions.

■ REFERENCES

(1) Kondratenko, E. V.; Peppel, T.; Seeburg, D.; Kondratenko, V. A.; Kalevaru, N.; Martin, A.; Wohlrab, S. Methane Conversion Into Different Hydrocarbons or Oxygenates: Current Status and Future Perspectives in Catalyst Development and Reactor Operation. *Catal. Sci. Technol.* **2017**, *7*, 366−381.

(2) Schwach, P.; Pan, X.; Bao, X. Direct Conversion of Methane to Value-Added Chemicals over Heterogeneous Catalysts: Challenges and Prospects. *Chem. Rev.* **2017**, *117*, 8497−8520.

(3) Karakaya, C.; Kee, R. J. Progress in the Direct Catalytic Conversion of Methane to Fuels and Chemicals. *Prog. Energy Combust. Sci.* **2016**, *55*, 60−97.

(4) Galadima, A.; Muraza, O. Revisiting the Oxidative Coupling of Methane to Ethylene in the Golden Period of Shale Gas: A Review. *J. Ind. Eng. Chem.* **2016**, *37*, 1−13.

(5) Wang, L.; Tao, L.; Xie, M.; Xu, G.; Huang, J.; Xu, Y. Dehydrogenation and Aromatization of Methane under Non-oxidizing Conditions. *Catal. Lett.* **1993**, *21*, 35−41.

(6) Spivey, J. J.; Hutchings, G. Catalytic Aromatization of Methane. *Chem. Soc. Rev.* **2014**, *43*, 792−803.

(7) Wang, D.; Lunsford, J. H.; Rosynek, M. P. Catalytic Conversion of Methane to Benzene over Mo/ZSM-5. *Top. Catal.* **1996**, *3*, 289−297.

(8) Tessonnier, J.-P.; Louis, B.; Rigolet, S.; Ledoux, M. J.; Pham-Huu, C. Methane Dehydro-Aromatization on Mo/ZSM-5: About the Hidden Role of Brønsted Acid Sites. *Appl. Catal., A* **2008**, *336*, 79−88.

(9) Ismagilov, Z. R.; Matus, E. V.; Tsikoza, L. T. Direct Conversion of Methane on Mo/ZSM-5 Catalysts to Produce Benzene and hydrogen: achievements and perspectives. *Energy Environ. Sci.* **2008**, *1*, 526−541.

(10) Nishikawa, Y.; Ogihara, H.; Yamanaka, I. Liquid-Metal Indium Catalysis for Direct Dehydrogenative Conversion of Methane to Higher Hydrocarbons. *ChemistrySelect* **2017**, *2*, 4572−4576.

(11) Koerts, T.; Deelen, M. J.; van Santen, R. A. Hydrocarbon Formation from Methane by a Low-Temperature Two-Step Reaction Sequence. *J. Catal.* **1992**, *138*, 101−114.

(12) Wu, M.-C.; Lenz-Solomun, P.; Goodman, D. W. Two-step, Oxygen-Free Route to Higher Hydrocarbons from Methane over Ruthenium Catalysts. *J. Vac. Sci. Technol., A* **1994**, *12*, 2205−2209.

(13) Guczi, L. Non-oxidative Methane Coupling over Co-Pt/NaY Bimetallic Catalysts. *Catal. Lett.* **1996**, *39*, 43−47.

(14) Wang, L.; Xu, Y.; Wong, S.-T.; Cui, W.; Guo, X. Activity and Stability Enhancement of MoHZSM-5-based Catalysts for Methane Non-Oxidative Transformation to Aromatics and C_2 Hydrocarbons: Effect of Additives and Pretreatment Conditions. *Appl. Catal., A* **1997**, *152*, 173−182.

(15) Amariglio, A.; Belgued, M.; Pareja, P.; Amariglio, H. Oxygen-free Conversion of Methane to Higher Hydrocarbons through a Dual-Temperature Two-Step Reaction Sequence on Platinum and Ruthenium: 1. Chemisorption of CH_4 at a Fixed Temperature. *J. Catal.* **1998**, *177*, 113−120.

(16) Tshabalala, T. E.; Coville, N. J.; Scurrell, M. S. Methane Dehydroaromatization over Modified Mn/H-ZSM-5 Zeolite Catalysts: Effect of Tungsten as a Secondary Metal. *Catal. Commun.* **2016**, *78*, 37−43.

(17) Belgued, M.; Pareja, P.; Amariglio, A.; Amariglio, H. Conversion of Methane into Higher Hydrocarbons on Platinum. *Nature* **1991**, *352*, 789−790.

(18) Soulivong, D.; Norsic, S.; Taoufik, M.; Coperet, C.; Thivolle-Cazat, J.; Chakka, S.; Basset, J.-M. Non-Oxidative Coupling Reaction of Methane to Ethane and Hydrogen Catalyzed by the Silica-Supported Tantalum Hydride:SiO_2Ta-H. *J. Am. Chem. Soc.* **2008**, *130*, 5044−5045.

(19) Guo, X.; Fang, G.; Li, G.; Ma, H.; Fan, H.; Yu, L.; Ma, C.; Wu, X.; Deng, D.; Wei, M.; Tan, D.; Si, R.; Zhang, S.; Li, J.; Sun, L.; Tang,

DOI: 10.1021/acscatal.8b00156
ACS Catal. 2018, 8, 2735−2740

Z.; Pan, X.; Bao, X. Direct, Nonoxidative Conversion of Methane to Ethylene, Aromatics, and Hydrogen. *Science* **2014**, *344*, 616−619.
(20) Gerceker, D.; Motagamwala, A. H.; Rivera-Dones, K. R.; Miller, J. B.; Huber, G. W.; Mavrikakis, M.; Dumesic, J. A. Methane Conversion to Ethylene and Aromatics on PtSn Catalysts. *ACS Catal.* **2017**, *7*, 2088−2100.
(21) Ertl, G.; Knozinger, H.; Schuth, F.; Weitkamp, J. *Handbook of Heterogeneous Catalysis: 3.1.2 Particle Size and Dispersion Measurements*, 2nd ed.; Wiley-VCH: Weinheim, Germany, 2008; Vol. *1*, pp 738−765.
(22) Benson, J. E.; Boudart, M. Hydrogen-Oxygen Titration Method for the Measurement of Supported Platinum Surface Areas. *J. Catal.* **1965**, *4*, 704−710.
(23) Baerlocher, C.; McCusker, L. B.; Olson, D. H. MFI - Pnma. *Atlas of Zeolite Framework Types*, 6th ed.; Elsevier Science: Amsterdam, The Netherlands, 2007; pp 212−213.
(24) Zhu, Z.; Lu, G.; Guo, Y.; Guo, Y.; Zhang, Z.; Wang, Y.; Gong, X.-Q. High Performance and Stability of the Pt-W/ZSM-5 Catalyst for the Total Oxidation of Propane: the Role of Tungsten. *ChemCatChem* **2013**, *5*, 2495−2503.
(25) Li, Y.; Li, D.; Wang, G. Methane Decomposition to CO_x-free Hydrogen and Nano-Carbon Material on Group 8−10 Base Metal Catalysts: a Review. *Catal. Today* **2011**, *162*, 1−48.
(26) Weckhuysen, B. M.; Rosynek, M. P.; Lunsford, J. H. Characterization of Surface Carbon Formed During the Conversion of Methane to Benzene over Mo/H-ZSM-5 Catalysts. *Catal. Lett.* **1998**, *52*, 31−36.
(27) Fila, V.; Bernauer, M.; Bernauer, B.; Sobalik, Z. Effect of Addition of a Second Metal in Mo/ZSM-5 Catalyst for Methane Aromatization Reaction under Elevated Pressures. *Catal. Today* **2015**, *256*, 269−275.
(28) Kimura, H.; Tsuto, K.; Wakisaka, T.; Kazumi, Y.; Inaya, Y. Selective Oxidation of Glycerol on a Platinum-Bismuth Catalyst. *Appl. Catal., A* **1993**, *96*, 217−228.
(29) Villa, A.; Campisi, S.; Chan-Thaw, C. E.; Motta, D.; Wang, D.; Prati, L. Bismuth Modified Au-Pt Bimetallic Catalysts for Dihydroxyacetone Production. *Catal. Today* **2015**, *249*, 103−108.
(30) Paffett, M. T.; Campbell, C. T.; Taylor, T. N. The Influence of Adsorbed Bi on the Chemisorption Properties of Pt(111): H_2, CO, and O_2. *J. Vac. Sci. Technol., A* **1985**, *3*, 812−816.
(31) Windham, R. G.; Koel, B. E.; Paffett, M. T. Studies of the Ensemble Size Requirements for Ethylene Adsorption and Decomposition on Platinum(111): Ethylene and Bismuth Coadsorption. *Langmuir* **1988**, *4*, 1113−1118.
(32) Gomez, R.; Feliu, J. M.; Aldaz, A. Effects of Irreversibly Adsorbed Bismuth on Hydrogen Adsorption and Evolution on Pt(111). *Electrochim. Acta* **1997**, *42*, 1675−1683.
(33) Pasti, I. A.; Mentus, S. V. Modification of Electronic Properties of Pt(111) Surface by Means of Alloyed and Adsorbed Metals: DFT Study. *Russian Journal of Physical Chemistry A* **2009**, *83*, 1531−1536.
(34) Greeley, J.; Jaramillo, T. F.; Bonde, J.; Chorkendorff; Norskov, J. K. Computational High-throughput Screening of Electrocatalytic Materials for Hydrogen Evolution. *Nat. Mater.* **2006**, *5*, 909−913.
(35) Hu, W.; Knight, D.; Lowry, B.; Varma, A. Selective Oxidation of Glycerol to Dihydroxyacetone over Pt-Bi/C Catalyst: Optimization of Catalyst and Reaction Conditions. *Ind. Eng. Chem. Res.* **2010**, *49*, 10876−10882.
(36) Vines, F.; Lykhach, Y.; Staudt, T.; Lorenz, M. P. A.; Papp, C.; Steinruck, H.-P.; Libuda, J.; Neyman, K. M.; Gorling, A. Methane Activation by Platinum: Critical Role of Edge and Corner Sites of Metal Nanoparticles. *Chem. - Eur. J.* **2010**, *16*, 6530−6539.
(37) Lin, Y.-Z.; Sun, J.; Yi, J.; Lin, J.-D.; Chen, H.-B.; Liao, D.-W. Energetics of Chemisorption and Conversion of Methane on Transition Metal Surfaces. *J. Mol. Struct.: THEOCHEM* **2002**, *587*, 63−71.
(38) Cheng, J.; Hu, P.; Ellis, P.; French, S.; Kelly, G.; Lok, C. M. Chain Growth Mechanism in Fischer−Tropsch Synthesis: a DFT Study of C-C Coupling over Ru, Fe, Rh, and Re Surfaces. *J. Phys. Chem. C* **2008**, *112*, 6082−6086.
(39) Yang, M.-L.; Zhu, Y.-A.; Fan, C.; Sui, Z.-J.; Chen, D.; Zhou, X.-G. DFT Study of Propane Dehydrogenation on Pt Catalyst: Effects of Step Sites. *Phys. Chem. Chem. Phys.* **2011**, *13*, 3257−3267.
(40) Wei, J.; Iglesia, E. Mechanism and Site Requirements for Activation and Chemical Conversion of Methane on Supported Pt Clusters and Turnover Rate Comparisons among Noble Metals. *J. Phys. Chem. B* **2004**, *108*, 4094−4103.
(41) Lukyanov, D. B.; Gnep, N. S.; Guisnet, M. R. Kinetic Modeling of Propane Aromatization Reaction over HZSM-5 and GaHZSM-5. *Ind. Eng. Chem. Res.* **1995**, *34*, 516−523.
(42) Vosmerikova, L. N.; Zaikovskii, V. I.; Volynkina, A. N.; Vosmerikov, A. V. Deactivation Features of Gallium-Containing Zeolites in the Propane Aromatization Process. *Pet. Chem.* **2017**, *57*, 85−92.
(43) Galvita, V.; Siddiqi, G.; Sun, P.; Bell, A. T. Ethane Dehydrogenation on Pt/Mg(Al)O and PtSn/Mg(Al)O Catalysts. *J. Catal.* **2010**, *271*, 209−219.
(44) Wegener, E. C.; Wu, Z.; Tseng, H.-T.; Gallagher, J. R.; Ren, Y.; Diaz, R. E.; Ribeiro, F. H.; Miller, J. T. Structure and Reactivity of Pt-In Intermetallic Alloy Nanoparticles: Highly Selective Catalysts for Ethane Dehydrogenation. *Catal. Today* **2018**, *299*, 146−153.
(45) Greeley, J.; Norskov, J. K. Combinatorial Density Functional Theory-Based Screening of Surface Alloys for the Oxygen Reduction Reaction. *J. Phys. Chem. C* **2009**, *113*, 4932−4939.
(46) Hook, A.; Massa, J. D.; Celik, F. E. Effect of Tin Coverage on Selectivity for Ethane Dehydrogenation over Platinum-Tin Alloys. *J. Phys. Chem. C* **2016**, *120*, 27307−27318.
(47) Wu, J.; Sharada, S. M.; Ho, C.; Hauser, A. W.; Head-Gordon, M.; Bell, A. T. Ethane and Propane Dehydrogenation over PtIr/Mg(Al)O. *Appl. Catal., A* **2015**, *506*, 25−32.
(48) Yu, Z.; Sawada, J. A.; An, W.; Kuznicki, S. M. PtZn-ETS-2: a Novel Catalyst for Ethane Dehydrogenation. *AIChE J.* **2015**, *61*, 4367−4376.
(49) Pasti, I.; Mentus, S. DFT Study of Adsorption of Hydrogen and Carbon Monoxide on Pt_xBi_{1-x}/Pt(111) Bimetallic Overlayers: Correlation to Surface Electronic Properties. *Phys. Chem. Chem. Phys.* **2009**, *11*, 6225−6233.
(50) Xiao, Y.; Greeley, J.; Varma, A.; Zhao, Z.-J.; Xiao, G. An Experimental and Theoretical Study of Glycerol Oxidation to 1,3-Dihydroxyacetone over Bimetallic Pt-Bi Catalysts. *AIChE J.* **2017**, *63*, 705−715.
(51) Xiao, Y.; Varma, A. Catalytic Deoxygenation of Guaiacol Using Methane. *ACS Sustainable Chem. Eng.* **2015**, *3*, 2606−2610.
(52) Amano, H.; Sato, S.; Takahashi, R.; Sodesawa, T. Dehydrogenation of Cyclohexene over Carbon Deposited on Alumina. *Phys. Chem. Chem. Phys.* **2001**, *3*, 873−879.
(53) McGregor, J.; Huang, Z.; Parrott, E. P.; Zeitler, J. A.; Nguyen, K. L.; Rawson, J. M.; Carley, A.; Hansen, T. W.; Tessonnier, J.-P.; Su, D. S.; Teschner, D.; Vass, E. M.; Knop-Gericke, A.; Schlogl, R.; Gladden, L. F. Active Coke: Carbonaceous Materials as Catalysts for Alkane Dehydrogenation. *J. Catal.* **2010**, *269*, 329−339.
(54) Nederlof, C.; Kapteijn, F.; Makkee, M. Catalysed Ethylbenzene Dehydrogenation in CO_2 or N_2-Carbon Deposits as the Active Phase. *Appl. Catal., A* **2012**, *417−418*, 163−173.
(55) Collett, C. H.; McGregor, J. Things Go Better with Coke: the Beneficial Role of Carbonaceous Deposits in Heterogeneous Catalysis. *Catal. Sci. Technol.* **2016**, *6*, 363−378.

DOI: 10.1021/acscatal.8b00156
ACS Catal. 2018, 8, 2735−2740